

Lawrence Berkeley National Laboratory

Recent Work

Title

Simulation of High Resolution Images of Wedge-Shaped Crystals

Permalink

<https://escholarship.org/uc/item/6225h37g>

Authors

Hetherington, C.

O'Keefe, M.A.

Kilaas, R.

Publication Date

1989



Lawrence Berkeley Laboratory

UNIVERSITY OF CALIFORNIA

Materials & Chemical Sciences Division

National Center for Electron Microscopy

Presented at the TMS Annual Meeting, Las Vegas, NV,
February 27–March 2, 1989, and published in the
Proceedings (*Computer Simulation of Electron
Microscope Diffraction and Images*)

Simulation of High Resolution Images of Wedge-Shaped Crystals

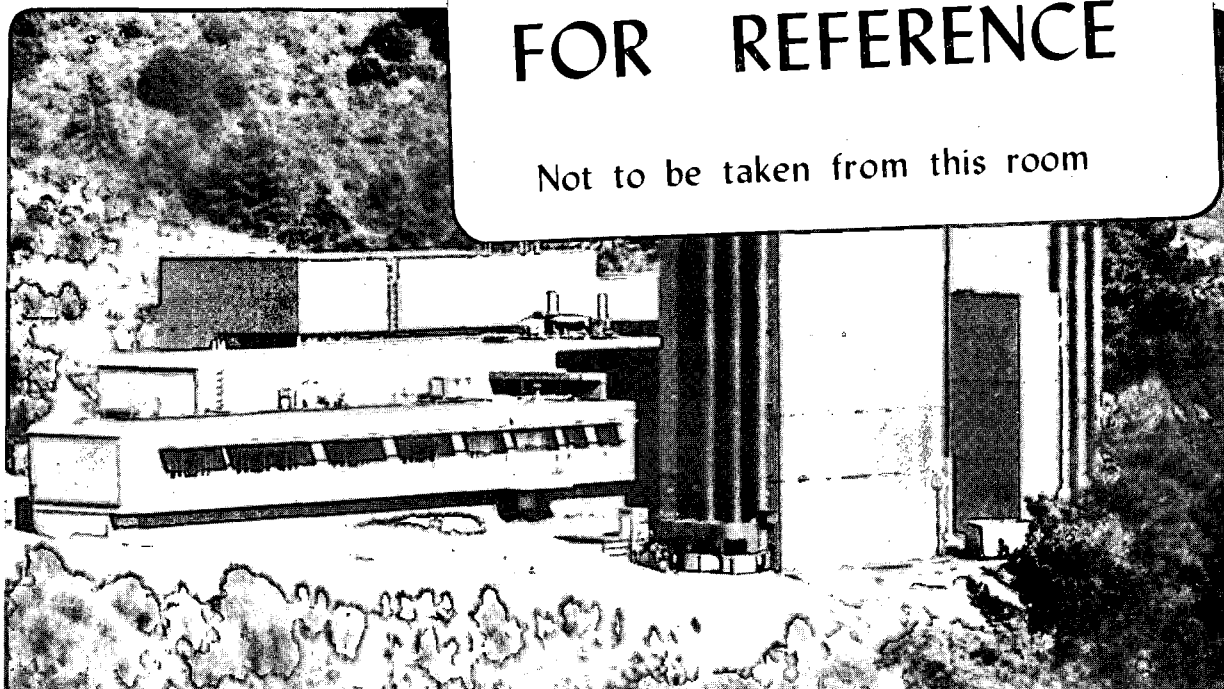
C. Hetherington, M.A. O'Keefe, and R. Kilaas

January 1989

U. C. Lawrence Berkeley Laboratory
Library, Berkeley

FOR REFERENCE

Not to be taken from this room



DISCLAIMER

This document was prepared as an account of work sponsored by the United States Government. While this document is believed to contain correct information, neither the United States Government nor any agency thereof, nor the Regents of the University of California, nor any of their employees, makes any warranty, express or implied, or assumes any legal responsibility for the accuracy, completeness, or usefulness of any information, apparatus, product, or process disclosed, or represents that its use would not infringe privately owned rights. Reference herein to any specific commercial product, process, or service by its trade name, trademark, manufacturer, or otherwise, does not necessarily constitute or imply its endorsement, recommendation, or favoring by the United States Government or any agency thereof, or the Regents of the University of California. The views and opinions of authors expressed herein do not necessarily state or reflect those of the United States Government or any agency thereof or the Regents of the University of California.

**Simulation of High Resolution Images
of Wedge-Shaped Crystals**

C. Hetherington, M.A. O'Keefe, and R. Kilaas

Materials Science Division
National Center for Electron Microscopy
University of California
Lawrence Berkeley Laboratory
Berkeley, CA 94720

Published in "Computer Simulation of Electron Microscope
Diffraction and Images" from TMS Annual Meeting
Las Vegas, NV. 2/27-3/2/89

This work was supported in part by the Director, Office of Energy Research, Office of Basic Energy Sciences, Materials Science Division of the U.S. Department of Energy under Contract No. DE-AC03-76SF00098.

1

SIMULATION OF HIGH RESOLUTION IMAGES OF WEDGE-SHAPED CRYSTALS

C. J. D. Hetherington, M. A. O'Keefe and R. Kilaas

National Center for Electron Microscopy
Lawrence Berkeley Laboratory
University of California
1 Cyclotron Rd., Berkeley, CA 94720.

Abstract

TEM specimens of semiconductor materials, prepared by cleaving on well-defined planes, have clean, flat surfaces and the regular wedge shape means that the thickness is directly related to the distance from the edge of the specimen. The form of the high resolution image varies across a single micrograph as the thickness and exit-surface height (i.e. focus) change, in a known way, across the specimen. Experimental images of these specimens are thus already well characterized and can be used to test the accuracy of simulated images under these conditions. This paper shows examples of experimental and simulated images and examines the success (or otherwise) of the matching for various computational procedures and model specimen parameters.

Introduction

2

To determine an atomic structure by high resolution electron microscopy, the standard procedure is to compare experimental images with the (simulated) images that would be expected for the various possible atomic models. However, high resolution images are sensitive not only to the atomic structure of the specimen but also other parameters, especially thickness of the specimen and defocus of the microscope (see e.g. (1) for a review). Often those parameters are not known exactly and images must be simulated for the estimated range of the possible imaging conditions before a match with the experimental image can be found.

There are certain specimens however which have well defined shapes that allow measurements or, at least, good estimates of thickness and defocus - namely, regular wedge shapes. One example is MgO whose smoke forms as perfect cubes with {100} faces. These have been used as TEM specimens and examined at high resolution by O'Keefe and coworkers (2). Earlier work by Uyeda and Nonoyama (3) made use of the cleavage on these {100} planes to produce similar 90° wedges to study extinction distances in MgO. A second material that allows the preparation of wedge-shaped TEM specimens was introduced by Kakibayashi and Nagata (4). In their work, GaAs wafers were cleaved along orthogonal {110} planes to form a 90° wedge through the thickness of a (001) wafer thus forming a cross section TEM specimen. The specimen can be viewed down the [100] zone in bright field (4,5) or at high resolution (6).

MgO and GaAs wedge specimens provide an opportunity to obtain experimental high resolution images that are already well characterized by their geometry in terms of thickness and defocus change into the wedge. These images should make it possible to test the accuracy of simulated images and to refine parameters such as absorption parameters, vibration amplitudes and even perhaps structure factor deviations due to bonding.

In this paper, the possible configurations for examining GaAs wedges are described, experimental images are presented from one such wedge and preliminary calculations produced by multislice and matrix calculations are shown.

Specimen Preparation

GaAs was chosen in this study since it cleaves along precise {110} planes often with a very low density of steps and seldom with any deviation from the {110} plane. The resulting wedges are bounded by two flat {110} planes. The 6 non-parallel {110} planes allow a number of different types of wedges to be made. Given sufficient resolution, some wedges can be viewed down several zone axes with the line of the wedge-edge maintained horizontal. Figure 1 illustrates some of these possibilities.

The details of the preparation are described elsewhere (7) but important points to be noted are as follows: The starting materials were wafers of GaAs with surface normals of [100] or [111]. Portions of the wafers were thinned down to around 100µm before cleaving on the {110} planes perpendicular to the wafer

surface. The cleaved planes were inspected under an optical microscope for flatness. The pieces chosen were mounted upright in silver epoxy glue on a slot grid.

Other semiconductor materials were also considered. Whereas compound semiconductors were found to be suitable, elemental semiconductors such as Si or Ge were found not to produce wedge shapes with surfaces on well-defined crystallographic planes.

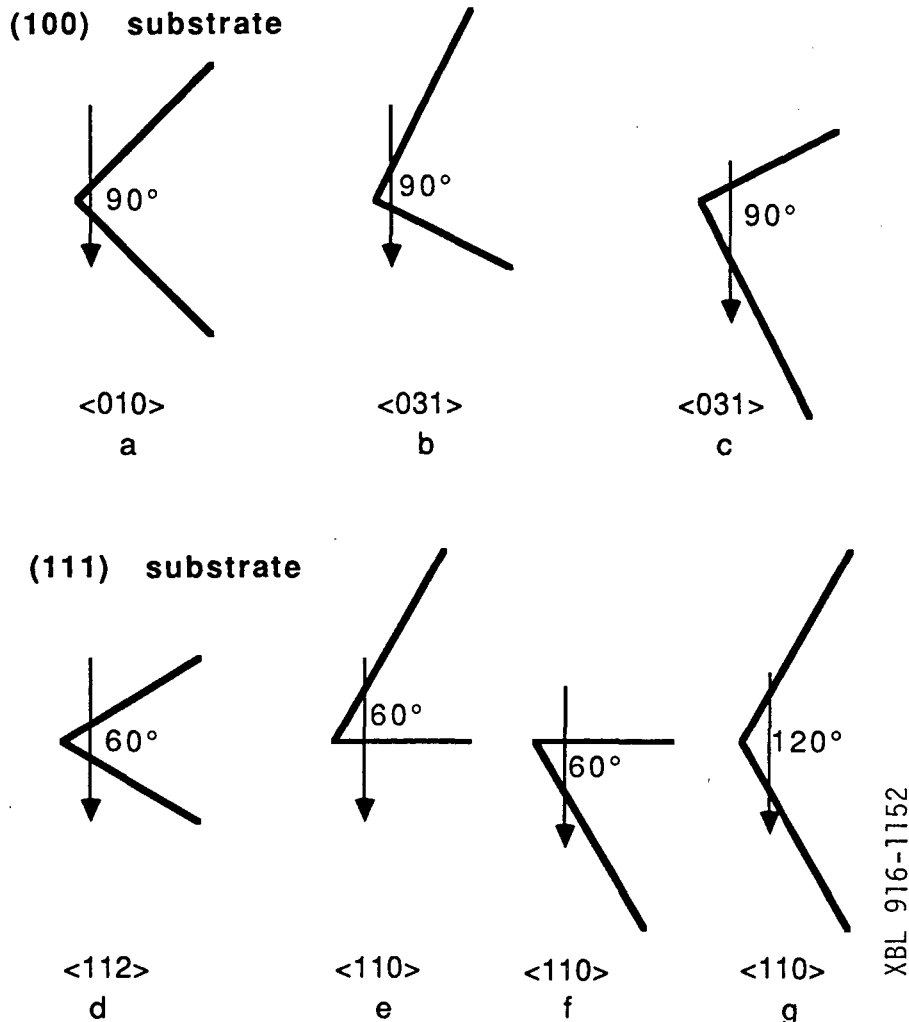
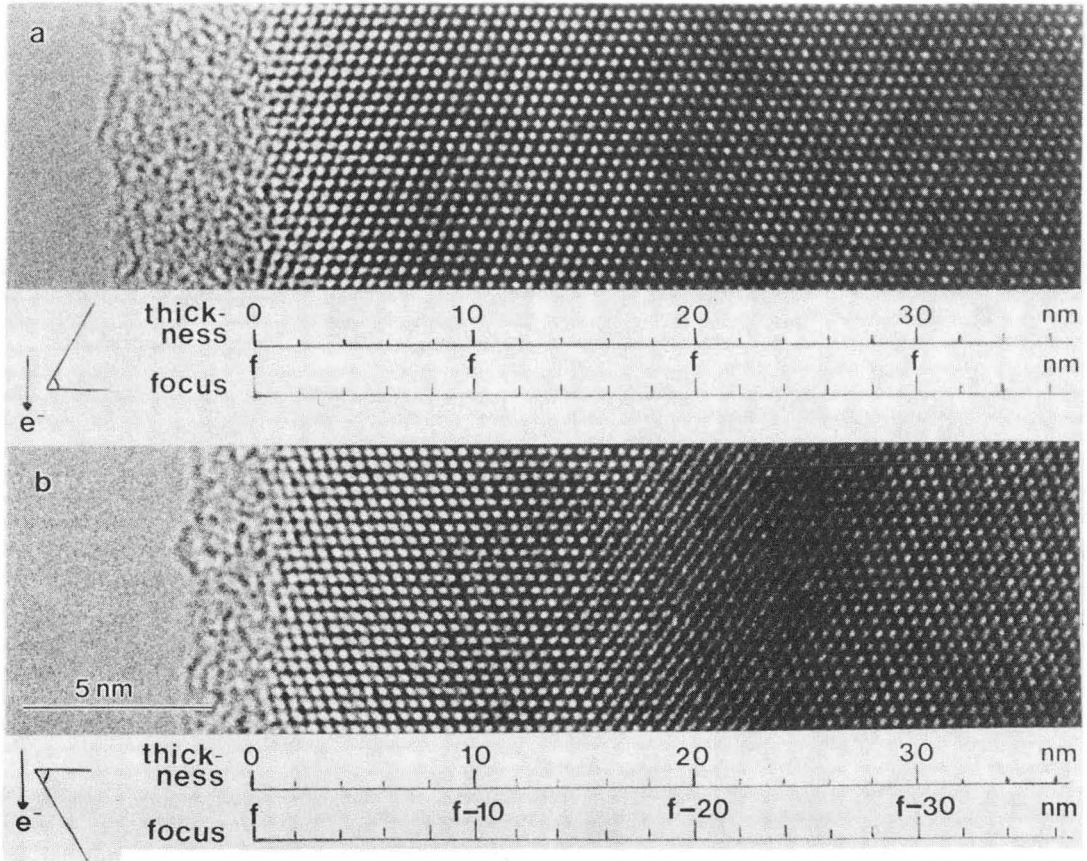


Fig.1 Possible configurations for observing GaAs wedge specimens. The cleaved faces lie on $\{110\}$ planes and the zones are indicated below each wedge.

Microscopy

The specimens were examined in a $\pm 40^\circ$ biaxial tilt holder at 800kV in the ARM-1000 at Berkeley. Large tilts were occasionally required to reach the zone axes and the height control of the specimen stage proved necessary as the wedge edge was sometimes located several hundred microns above or below the slot grid. Tilting precisely to the zone was relatively straightforward since the proximity of thick material to the edge of the specimen both prevents buckling of the specimen and allows Kikuchi bands



XBB 902-1486

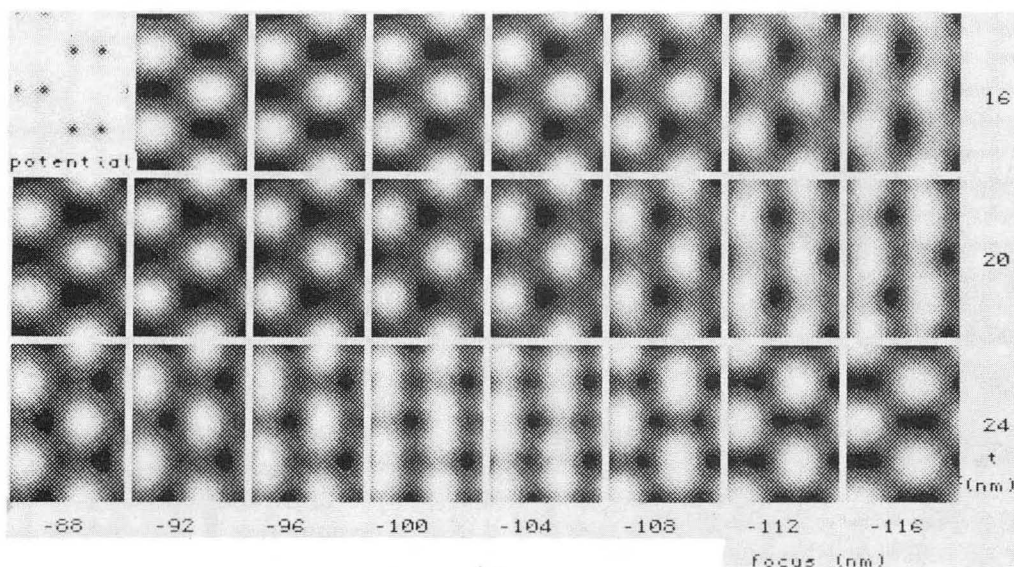
Fig.2 Images of the same 60° GaAs wedge viewed down different 110 directions. a) horizontal exit surface leading to constant focus (as in fig.1e), b) inclined exit surface leading to varying focus (as in fig.1f) (The sample was left in air for several weeks between recording the images which explains the thicker amorphous layer in a.)

(rather than diffraction spot intensities) to be used to align the pole.

Figure 2 shows two high resolution images of a 60° wedge. The thickness is determined by the geometry of the specimen and the distance from the wedge edge. This measurement assumes that there is no rounding or blunting of the crystalline edge but that it does remain sharp. Even so, the crystalline edge is obscured by the amorphous layer and this introduces an uncertainty of perhaps 1nm into the thickness measurement. Similarly, the change into the wedge is accurately known but the absolute value at the edge can only be estimated to within a few tens of nanometers. The values of focus change and thickness are indicated on the images.

Examination of the experimental images of the two 60° wedges, having constant (a) and varying (b) focus into the wedge, reveals one significant difference between the images. A contrast reversal at around 20nm is present in the varying-focus image and

is seen most clearly in the $\{111\}$ fringes that run normal to the direction of the wedge edge. That the thickness does not have a large effect on the image is explained by calculations which show that the relative phase differences between 000 and the 111 reflections do not vary greatly up to 35nm. The simulated images in figure 3 show that the lower limit for the focus in fig.2a must be around -92nm (In fact, since the Fourier period of the 111 planes in GaAs at 800kV is over 200nm, there is a very wide range of possible values for the focus of the image of the crystalline material in fig.2a. However, the image of the amorphous material indicates a focus closer to Scherzer at -55nm) For fig.2b, the contrast reversal in the GaAs image can be explained by, say, a focus value of -108nm at 16nm thickness and a focus value of -116nm at 24nm thickness (see fig.3).



XBB 902-1485

Fig.3 Simulated images of GaAs calculated using the NCEMSS multislice routine for varying thickness and defocus.

Image Simulations

Some preliminary image simulations have been performed to compare matrix and multislice dynamical scattering formulations and to observe effects of adding vibration or absorption to the calculations.

The exit wavefunctions (real and imaginary components of diffracted beams) were calculated using the "SHRLI" multislice program (1), the "NCEMSS" multislice program (8) or a matrix (Bloch wave) program (9). The high resolution images were calculated using the "SHRLI" (1) imaging routine. These are run on the NCEM computing facility (10) and images are output on a laserwriter.

The input structure for GaAs in both the matrix and multislice calculations used the standard values for unit cell dimensions (lattice parameter = 0.565nm) and for the atomic coordinates. The scattering factors for Ga and As (isolated atoms) were taken from (11) and the values for the Debye-Waller factors at 295K

were taken from (12) (0.0064nm^2 for Ga and 0.0069nm^2 for As). The calculations were performed for 800kV electrons.

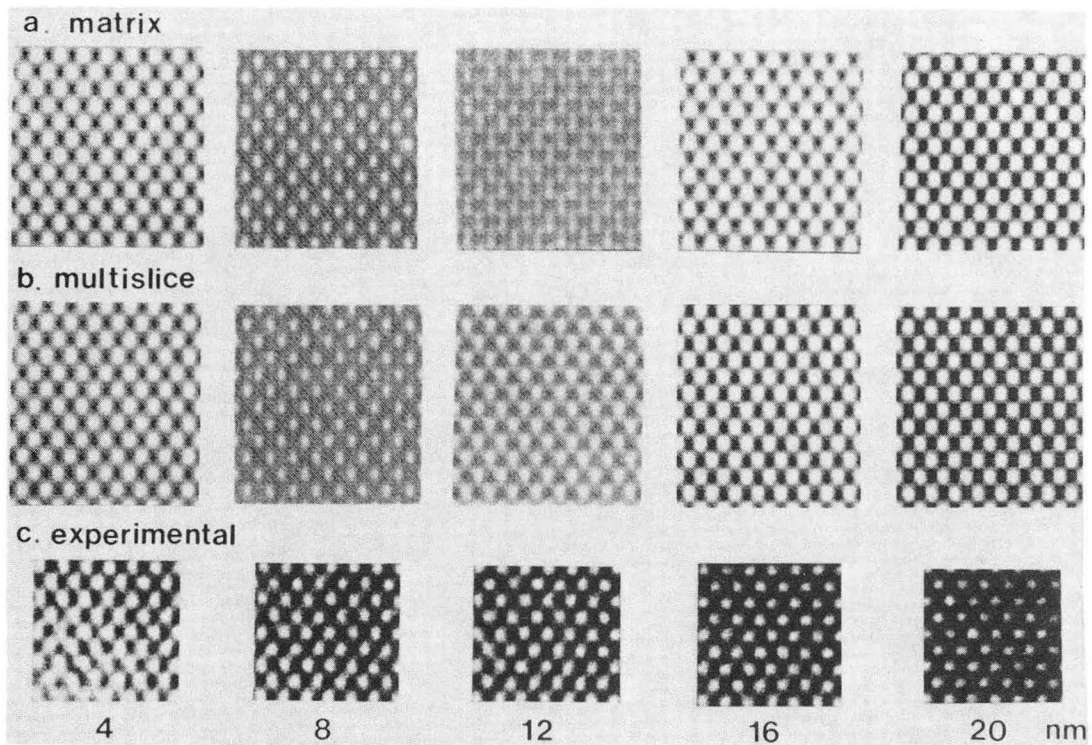
In the matrix calculations, 247 beams were used which covered an area in reciprocal space out to a radius of 35nm^{-1} . In matrix calculations, it is important to use enough beams to obtain the required accuracy. In this case, the number of beams was limited by the program to 256 or less. However, the accuracy of the calculation was tested by comparing the thickness of the first maximum of the central beam (000) as a function of the number of beams used in the calculation; the value had almost leveled off at around 15nm (without absorption) at 247 beams. The multislice calculations produced a value of around 14.5nm for the first maximum when beams out to 30nm^{-1} were included. The experimental observation of the first maximum in bright field intensity was at a thickness of $14\pm 1\text{nm}$.

In the multislice calculations, 561 beams were used corresponding to an area in reciprocal space of radius $g = 40\text{nm}^{-1}$; the 2267 phase grating coefficients extended to 80nm^{-1} . The projected potential was calculated for the whole unit cell as seen in the $\langle 110 \rangle$ direction and a single slice was used of thickness 0.400nm. (In fact, in the $\langle 110 \rangle$ direction, there are two layers of atoms having different projections; however, using two different slices corresponding to these two layers made no discernable difference to the calculated images.)

The exit wavefunctions were output for thicknesses of 4, 8, 12, 16 and 20nm and images calculated using the following parameters described in (13): accelerating voltage = 800kV, $C_s = 2.0\text{mm}$, defocus = -55nm, focus spread = 15nm, beam divergence semiangle = 0.75mrad, objective aperture radius = 5.5nm^{-1} . Images were output onto a laserwriter using values of intensity of 1.6 for white and 0.4 for black (an intensity of 1 represents the incident illumination).

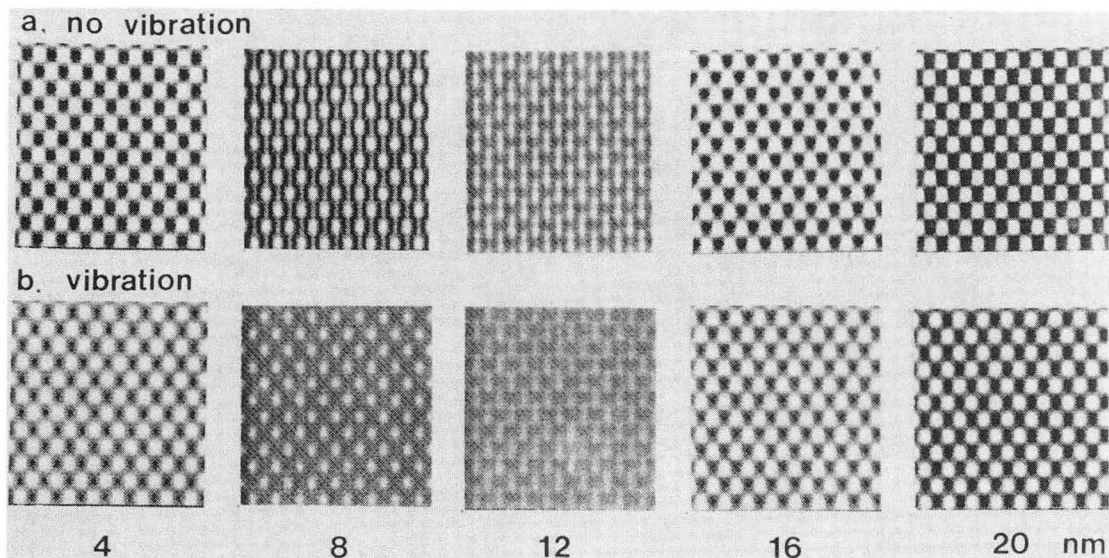
Discussion

Figure 4 shows for comparison two sets of images of GaAs simulated using different methods and a third set obtained experimentally. Note the difference in the image character between figures 4a and b at the (near) minimum contrast thickness of 12nm due presumably to the slight difference in extinction lengths of the two methods. Apart from this discrepancy, the images produced by the two methods bear a close resemblance to each other. The contrast in the experimental images however shows less variation with thickness than the contrast of the simulated images. The explanation for this may be the non-linearity of the response of the photographic emulsion in the negative for the particular exposure used.



XBB 902-1484

Fig.4 Images from a) multislice, b) matrix formulations and c) experiment (from fig.2a); thickness as marked applies to the center - lower left is $\sim 1.5\text{nm}$ thinner and upper right is $\sim 1.5\text{nm}$ thicker, (vibration of half-width 0.05nm , zero absorption).



XBB 902-1483

Fig.5 Images calculated (matrix) for vibrations of the specimen with a Gaussian of halfwidth 0.0nm or 0.05nm .

Since mechanical instabilities at the specimen generally limit the detail that is recorded in TEM micrographs to a certain value ($\sim 0.11\text{nm}$ in the ARM (13)), vibrations need to be included in simulations to attenuate those higher spatial frequencies. This

is especially important where cross-aperture (or $g, -g$) interference is substantial. In figure 5a, a $\{220\}$ fringe component is visible in the simulated image at 8nm thickness but it is suppressed by the inclusion of vibrations in figure 5b. When compared with the experimental image (figure 4c) clearly the simulated image that includes vibration has the closer resemblance. The effect at other thicknesses is to decrease the contrast.

The absorption was modelled (see figure 6) using an imaginary component of the potential that was a function of g (the spatial frequency) as follows:

$$\frac{V_g^i}{V_g} = a + bg \quad (a = 0.05, b = 0.005\text{nm}, g \text{ in nm}^{-1})$$

These values of a and b are close to those used in work on bright field intensities in GaAs (5). (Since the inelastically scattered electrons undergo elastic scattering themselves, a more rigorous method would include this contribution to the lattice image as in (14).) Inspection of the images shows no effect up to 8nm and, as expected, a reduction in intensity of the images above 12nm. Unfortunately, level of intensity is not the ideal parameter to match quantitatively with experiment in the case of lattice images; if absorption were to change the image character, then it might be possible and indeed necessary to model.

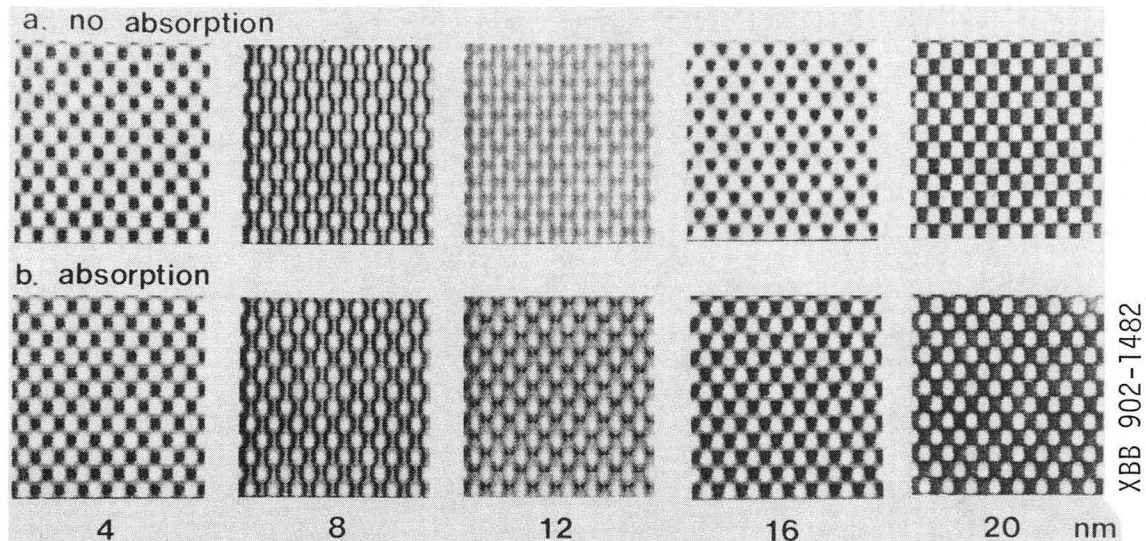


Fig.6 Images of GaAs calculated using the matrix formulation (and not including vibration): a) with absorption and b) without absorption.

Conclusion

These preliminary calculations and experimental results show that wedges afford an opportunity to obtain images in which the thickness and focus change are already well calibrated. The "calibrated" experimental images may prove useful for comparing assessing computational methods and, in some cases, scattering or

imaging parameters. GaAs offers a number of possible wedge configurations. However, the images of GaAs down [110] at 800kV show very little variation with thickness and defocus and this line of research might be more fruitful at lower voltages and using other materials where the images are more sensitive to thickness and defocus.

Acknowledgement

This work is supported by the Director, Office of Energy Research, Office of Basic Energy Science, Materials Science Division of the U.S. Department of Energy under contract No. DE-AC03-76SF00098. Useful discussions with P. A. Buffat are gratefully acknowledged.

References

1. M. A. O'Keefe, P. R. Buseck, and S. Iijima, "Computed Crystal Structure Images for High Resolution Electron Microscopy," Nature, 274 (1978) 322-324.
2. M. A. O'Keefe, J. C. H. Spence, J. L. Hutchison, and W.G. Waddington, "HREM Profile Image Interpretation in MgO Cubes," Proc. 43rd Annual Meeting of Electron Microscopy Society of America, ed. G. W. Bailey (San Francisco Press, CA) (1985) 64-65.
3. R. Uyeda and M. Nonoyama, "Electron Microscope Study on the Extinction and Absorption of 100kV Electrons in Magnesium Oxide Single Crystals," Jpn. J. Appl. Phys., 7 (1965) 498-512.
4. H. Kakibayashi and F. Nagata, "Composition Dependence of Equal Thickness Fringes in an Electron Microscope Image of GaAs/Al_xGa_{1-x}As Multilayer Structure," Jpn. J. Appl. Phys., 24 (1985) L905-L907.
5. C. J. D. Hetherington and D. J. Eaglesham, "Compositional Studies Of Semiconductor Alloys by Bright Field Electron Microscope Imaging Of Wedged Crystals," Mat. Res. Soc. Symp. Proc., ed. J. D. Dow and I. K. Schuller, (Pittsburgh, PA: Materials Research Society, 1987) 77 473-478.
6. P. A. Buffat, P. Stadelmann, J. D. Ganière, D. Martin, and F. K. Reinhart, "HREM and REM observations of multiquantum well structures (AlGaAs/GaAs)," Inst. Phys. Conf. Ser., (IOP Publishing Ltd. London, UK) 87 (1987) 207-212
7. C. J. D. Hetherington, "Preparation of Semiconductor Cross Sections by Cleaving," Mat. Res. Soc. Symp. Proc., ed. J. C. Brawman, R. M. Anderson, and M. L. McDonald (Pittsburgh, PA: Materials Research Society, 1988) 115 143-148.
8. R. Kilaas, "Interactive Simulation of High Resolution Electron Micrographs", Proc. 45th Annual Meeting of Electron Microscopy Society of America, ed. G. W. Bailey (San Francisco Press, CA) (1987) 66-69.

9. The Bloch wave computer program was written by J. R. Baker and R. Vincent of H. H. Wills Physics Laboratory, Bristol University, U.K., (1983); the output for imaging by SHRLI was added by D. J. Eaglesham (1986).
10. R. Kilaas and M. A. O'Keefe, "The National Center for Electron Microscopy Integrated Hardware/Software system for Interactive Analysis of Transmission Electron Microscope Images," to be published in the proceedings of Scanning/EM West Conference, Long Beach, CA 1989.
11. P. A. Doyle and P. S. Turner, "Relativistic Hartree-Fock X-ray and Electron Scattering Factors," Acta Cryst., A24 (1968) 390-397.
12. J. S. Reid, "Debye-Waller Factors of Zinc-Blende-Structure Materials - A Lattice Dynamical Comparison," Acta Cryst., A39 (1983) 1-13.
13. C. J. D. Hetherington, E. C. Nelson, K. H. Westmacott, R. Gronsky, and G. Thomas, "The Berkeley Atomic Resolution Microscope - An Update," to be published in Mat. Res. Soc. Symp. Proc., ed. W. Krakow, F. A. Ponce, and D. J. Smith, (Pittsburgh, PA: Materials Research Society, 1989) 139.
14. C. B. Boothroyd and W. M. Stobbs, "The Contribution of Inelastically Scattered Electrons to High Resolution Images of (Al,Ga)As/GaAs Heterostructures," Ultramicroscopy 26 (1988) 361-376.

LAWRENCE BERKELEY LABORATORY
UNIVERSITY OF CALIFORNIA
INFORMATION RESOURCES DEPARTMENT
BERKELEY, CALIFORNIA 94720